

Simulation of Human Head Exposed to Handset Using Hybrid NFM/MoM Techniques

Lei Zhao^{#1}, Ke-Li Wu^{#2}

[#]The Department of Electronic Engineering, The Chinese University of Hong Kong, China

¹leizhao@ee.cuhk.edu.hk

²klwu@ee.cuhk.edu.hk

^{*}The Department of Mathematics, Xuzhou Normal University, Xuzhou, China

Abstract—The head of the user of a mobile telephone is modeled by a two-layered prolate excited by the near field of a patch antenna. A hybrid Null field method / Method of moments (NFM/MoM) numerical method is investigated in this paper. NFM is used to solve the scattering problem from the head model, and the MoM using the Rao-Wilton Glisson (RWG) basis functions is applied to model the dipole antenna by distributing a voltage source on a virtual surface lying inside the antenna physical surface, in which the delta-function generator is used to model the feed point. The coupling between the head model and a finite-length dipole antenna is considered by an iteration procedure. The accuracy and efficiency of the proposed algorithm are verified by comparing numerical results with other available data.

I. INTRODUCTION

The interaction of EM radiation with humans head has raised public concern about potential health effects and the medical use of radio-frequency (RF) and microwave radiation [1, 2]. On the other hand, the effect of the head on the performance of the mobile phone antenna motives us to study the interactions between mobile communications handsets and the human head.

It is of great importance to seek efficient solutions to electromagnetic (EM) problem from human head combined with mobile phone antennas. The MoM [3] and FDTD algorithms [4, 5] are widely used for analyzing the interaction between human head and mobile phone antennas. NFM developed by Waterman [6-8] have been proposed, especially to improve the numerical stability in computations for dielectric objects with extreme geometries and multilayered objects [9-11].

In this paper, a hybrid method was investigated that allows more efficient analysis of situations involving a multilayered prolate spheroidal head model exposed to a handset antenna. The problem is divided into separate two regions: source region and scatterer region as shown in Fig. 1. MoM is used to solve the source region including handset antenna, NFM is used to solve the scatterer region including the head model, and an iteration procedure is used for the coupling of the two regions. Initially, the source region is solved for the induced current, excluding the effect of scatter region. The fields due to the induced current are then used as excitation sources for the scattering problem from head model. The induced currents in scatter region are used to compute the back-scattered fields

on the surface of source region, which become supplementary excitations for source region. The MoM is then rerun to evaluate the induced currents on the source region due to both the source excitation region and the induced equivalent current sources from scatter region. An iterative procedure was then used to obtain convergence of the results for the interaction between the regions.

The significance of this hybrid approach is that it not only provides an effective approach for fast assessment of the SAR specification for a given handset antenna design, by incorporating with an appropriate measurement setup for measuring the electric field outside a physical prolate head model, it can also lead to a fast SAR measurement system without using the semi-open phantom and the expensive robotic arm for the mobile phone industry.

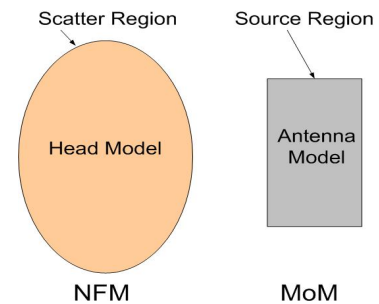


Fig. 1. Geometry model of NFM scatterer region and MoM source region

II. THEORY AND METHOD

The hybrid method starts by calculating the surface current in source region excluding the scatterer region. For a metal strip antenna in free space, the surface currents are first expanded by RWG basis function in the form

$$\bar{J} = \sum_{n=1}^{N_{MoM}} I_n \Lambda_n \quad (1)$$

where $\{\Lambda_n\}_{n=1}^{N_{MoM}}$ are the RWG basic functions [3] and N_{MoM} is the total number of unknowns in the source region. By applying the MoM, one can obtain an linear equations with unknown current coefficients as

$$\bar{Z} \cdot \bar{I} = \bar{V} \quad (2)$$

To account for the primary voltage source, the so-called delta function generator is used [12]. Supposing the voltage generator is associated with cell m whose edge length is l_m ,

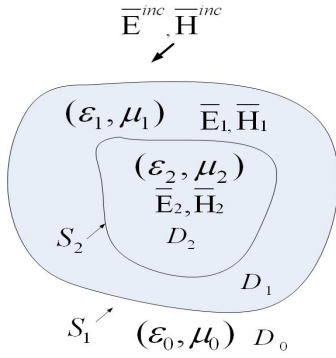


Fig. 2. Scattering problem form two layered dielectric object

all the entries in the voltage vector \bar{V} in (2) will be zero except element m whose value V_m , where is the applied voltage at the source gap. The induced currents can be obtained by solving matrix equation (2). The antenna impedance is then calculated by

$$Z_A = \frac{V_m}{I_m^2} \quad (3)$$

We consider EM scattering problem form two layered dielectric head model with permittivity and permeability (ϵ_1, μ_1) and (ϵ_2, μ_2) , respectively, which is in homogeneous space which is characterized by the parameters (ϵ_0, μ_0) , as shown in Fig. 2. According to the equivalence principle, the problem can be solved by considering two simpler equivalent problems, an internal equivalent problem and an external equivalent problem, respectively. Then, we can obtain the general null field equations

$$\begin{aligned} & \nabla \times \int_{S_1} (-\bar{J}_{1m}) \cdot \bar{G}(k_0, \bar{r}, \bar{r}') ds' \\ & + \frac{i}{\omega \epsilon_0} \nabla \times \nabla \times \int_{S_1} (-\bar{J}_{1e}) \cdot \bar{G}(k_0, \bar{r}, \bar{r}') ds' = -\bar{E}^{inc} \quad (4) \\ & \bar{r} \in D_{in} = D_1 \cup D_2 \cup S_2 \\ & -\nabla \times \int_{S_1} (-\bar{J}_{1m}) \cdot \bar{G}(k_1, \bar{r}, \bar{r}') ds' - \frac{i}{\omega \epsilon_1} \nabla \times \nabla \times \int_{S_1} \bar{J}_{1e} \\ & \cdot \bar{G}(k_1, \bar{r}, \bar{r}') ds' + \nabla \times \int_{S_2} (-\bar{J}_{2m}) \cdot \bar{G}(k_1, \bar{r}, \bar{r}') ds' \quad (5) \\ & + \frac{i}{\omega \epsilon_1} \nabla \times \nabla \times \int_{S_2} \bar{J}_{2e} \cdot \bar{G}(k_1, \bar{r}, \bar{r}') ds' = 0, \bar{r} \in D_0 \cup D_2 \end{aligned}$$

where \bar{J}_{1m} , \bar{J}_{1e} , and \bar{J}_{2m} , \bar{J}_{2e} are the equivalent electric current and magnetic current on surface S_1 and S_2 , respectively.

$\bar{G}(\bar{r}, \bar{r}') = \frac{e^{ik_0|\bar{r}-\bar{r}'|}}{4\pi|\bar{r}-\bar{r}'|} \bar{I}$ are the dyadic green function of free space.

To obtain an approximate solution of the null field equations (4) and (5), the surface equivalent currents are approximated by the complete set of regular VSWF's as [13]

$$\begin{pmatrix} \bar{J}_{1m}(\bar{r}') \\ \bar{J}_{1e}(\bar{r}') \end{pmatrix} = \sum_{\mu=1}^N c_{1\mu}^N \begin{pmatrix} -\hat{n}_1(\bar{r}') \times \bar{M}_\mu^1(k_1 \bar{r}') \\ -i \sqrt{\frac{\epsilon_1}{\mu_1}} \hat{n}_1(\bar{r}') \times \bar{N}_\mu^1(k_1 \bar{r}') \end{pmatrix} + d_{1\mu}^N \begin{pmatrix} -\hat{n}_1(\bar{r}') \times \bar{N}_\mu^1(k_1 \bar{r}') \\ -i \sqrt{\frac{\epsilon_1}{\mu_1}} \hat{n}_1(\bar{r}') \times \bar{M}_\mu^1(k_1 \bar{r}') \end{pmatrix} \quad (6)$$

$$\begin{aligned} & + \tilde{c}_{1\mu}^N \begin{pmatrix} -\hat{n}_1(\bar{r}') \times \bar{M}_\mu^2(k_1 \bar{r}') \\ -i \sqrt{\frac{\epsilon_1}{\mu_1}} \hat{n}_1(\bar{r}') \times \bar{N}_\mu^2(k_1 \bar{r}') \end{pmatrix} + \tilde{d}_{1\mu}^N \begin{pmatrix} -\hat{n}_1(\bar{r}') \times \bar{N}_\mu^2(k_1 \bar{r}') \\ -i \sqrt{\frac{\epsilon_1}{\mu_1}} \hat{n}_1(\bar{r}') \times \bar{M}_\mu^2(k_1 \bar{r}') \end{pmatrix} \\ & \begin{pmatrix} \bar{J}_{2m}(\bar{r}') \\ \bar{J}_{2e}(\bar{r}') \end{pmatrix} = \sum_{\mu=1}^N c_{2\mu}^N \begin{pmatrix} -\hat{n}_2(\bar{r}') \times \bar{M}_\mu^1(k_2 \bar{r}') \\ -i \sqrt{\frac{\epsilon_2}{\mu_2}} \hat{n}_2(\bar{r}') \times \bar{N}_\mu^1(k_2 \bar{r}') \end{pmatrix} \quad (7) \\ & + d_{2\mu}^N \begin{pmatrix} -\hat{n}_2(\bar{r}') \times \bar{N}_\mu^1(k_2 \bar{r}') \\ -i \sqrt{\frac{\epsilon_2}{\mu_2}} \hat{n}_2(\bar{r}') \times \bar{M}_\mu^1(k_2 \bar{r}') \end{pmatrix} \end{aligned}$$

where N is a truncation number of combined index μ , $\mu = 1, 2, \dots, N$ when $n = 1, 2, \dots, N_{rank}$, $m = -n, \dots, n$ and N_{rank} is the maximum expansion order of azimuthal modes.

Considering the general null field equations **Error! Reference source not found.** and (5), one can expand the incident field $\bar{E}^{inc}(\bar{r})$ and the dyad green function $\bar{G}(\bar{r}, \bar{r}')$ with the vector spherical wave functions (VSWF's) [14] as

$$\bar{E}^{inc} = \sum_{n=1}^{\infty} \sum_{m=-n}^n \left\{ a_{nm} \bar{M}_{nm}^1(k_0 \bar{r}) + b_{nm} \bar{N}_{nm}^1(k_0 \bar{r}) \right\} \quad (8)$$

$$\bar{G}(k, \bar{r}, \bar{r}') = ik \sum_{n=0}^{\infty} \sum_{m=-n}^n (-1)^m \left\{ \begin{aligned} & \bar{M}_{n(-m)}^{(3-p)}(k \bar{r}') \bar{M}_{nm}^p(k \bar{r}) \\ & + \bar{N}_{n(-m)}^{(3-p)}(k \bar{r}') \bar{N}_{nm}^p(k \bar{r}) \\ & + \bar{L}_{n(-m)}^{(3-p)}(k \bar{r}') \bar{L}_{nm}^p(k \bar{r}) \end{aligned} \right\} \quad (9)$$

where

$$p = \begin{cases} 1, & |\bar{r}| < |\bar{r}'| \\ 2, & |\bar{r}| > |\bar{r}'| \end{cases} \quad (10)$$

and \bar{L}_{nm}^p , \bar{M}_{nm}^p and \bar{N}_{nm}^p are there VSWF's. Using the orthogonality of the VSWF's on an inscribed spherical surface, one can obtain

$$\bar{Q}_1^{21}(k_0, k_1) \bar{i}_1 + \bar{Q}_1^{22}(k_0, k_1) \bar{i}_1 = -\bar{e} \quad (11)$$

$$-\bar{i}_1 + \bar{Q}_2^{11}(k_1, k_2) \bar{i}_2 = 0 \quad (12)$$

$$\bar{i}_1 + \bar{Q}_2^{21}(k_1, k_2) \bar{i}_2 = 0 \quad (13)$$

where $\bar{i}_1 = [c_{1\mu}^N, d_{1\mu}^N]^T$, $\bar{i}_1 = [\tilde{c}_{1\mu}^N, \tilde{d}_{1\mu}^N]^T$, $\bar{i}_2 = [c_{2\mu}^N, d_{2\mu}^N]^T$, and as before, $\bar{e} = [a_\nu, b_\nu]^T$ is the vector containing the expansion coefficients of incident field. Solving the system of matrix equations, the unknown coefficients \bar{i}_1 , \bar{i}_1 , and \bar{i}_2 can be obtained.

Then, the electromagnetic field inside and outside of the head model can be computed. When an antenna is presented in the vicinity of the double layered prolate head model, the scattering field also represents as the secondary excitation

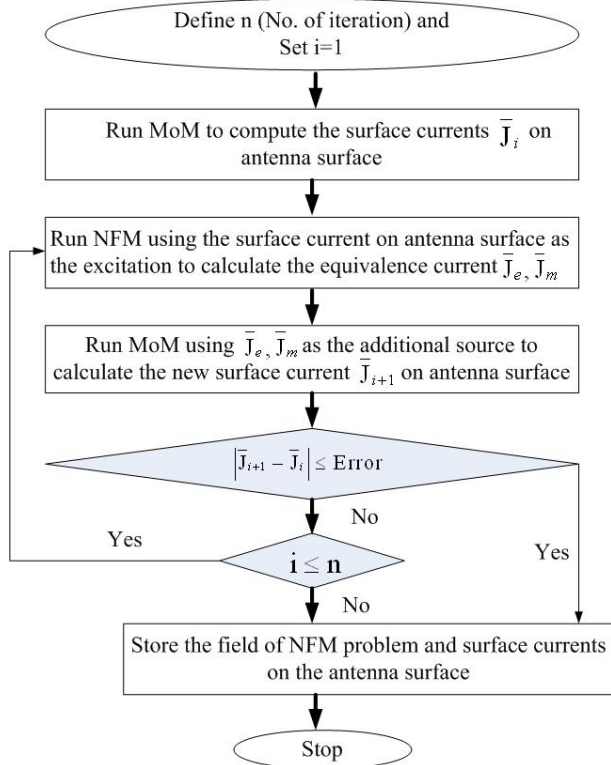


Fig. 3 Flow chart for the hybrid NFM/MoM algorithm

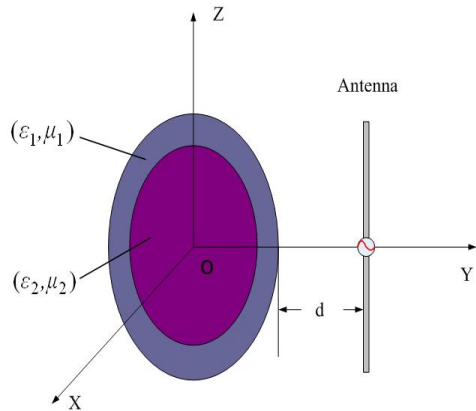


Fig. 4. Geometry of double layered prolate head model exposed to a dipole antenna.

source to the antenna. By taking into account of the prime and the secondary excitations to the antenna, an updated current distribution on the surface of the antenna can be obtained using the MoM. The procedure can be repeated to obtain a steady state solution, as shown in the flowchart Fig. 3.

III. NUMERICAL RESULTS

To illustrate the accuracy and efficiency of the NFM, we first consider the EM scattering from a human head model exposed to a half wavelength dipole antenna, as shown in

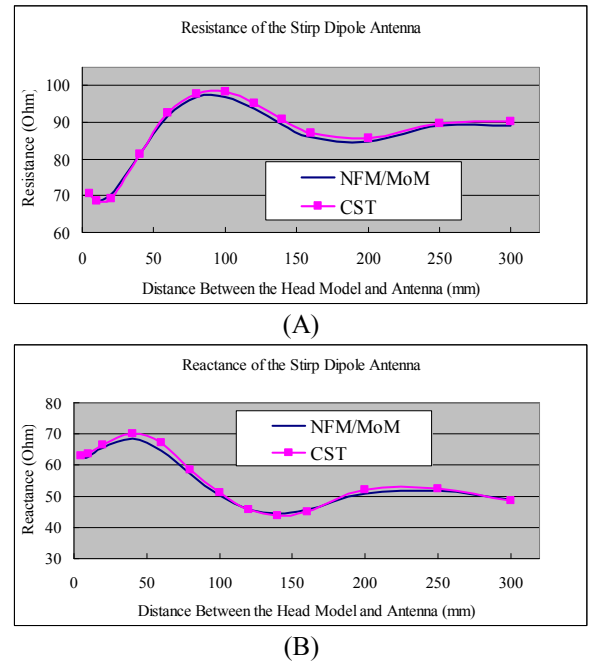


Fig. 5. Input impedance of a dipole antenna adjacent to a double layered prolate versus separation Distance. (A) Resistance of dipole antenna; (B); Reactance of dipole antenna.

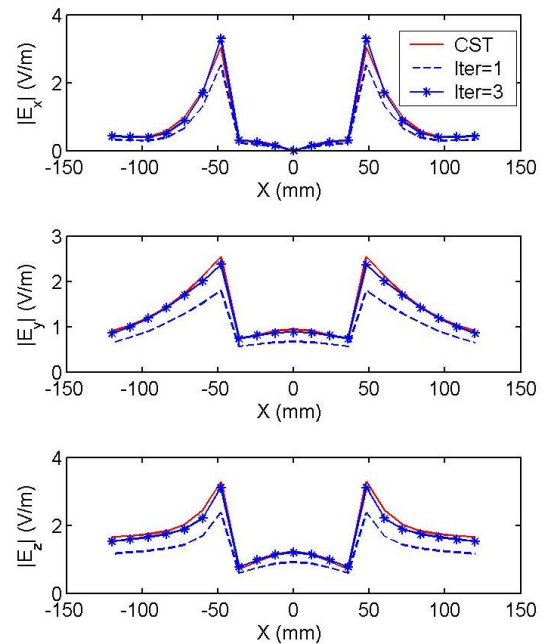


Fig. 6. Field distribution on the line of $y = 40\text{mm}$, $z = 66\text{mm}$ from the prolate head model adjacent to a half wavelength dipole antenna with separation distance of 20mm. Number of iteration = 1, and 3, respectively.

Fig.4. The head model used is a layered dielectric prolate, whose major semi-axial lengths of outer and inner layer are 100 mm and 98 mm, respectively. The ellipticity of the prolate spheroid is 0.8. The permittivity, conductivity and mass density parameters of the dielectric layer and the core are $\epsilon_{r1} = 5$, $\sigma_1 = 0.05\text{ S/m}$, $\rho_1 = 1000\text{ kg/m}^3$, $\epsilon_{r2} = 42$,

$\sigma_2 = 0.99 \text{ S/m}$, and $\rho_2 = 1000 \text{ kg/m}^3$, respectively. It can be seen from Fig. 5 that very good agreement between the results obtained from the CST software [15] and the proposed hybrid approach can be observed. To show the speed of convergence of the hybrid approach, the electric field intensity calculated in the first three iterations alone an observation line are compared with the full wave CST simulation in Fig. 6. It shows that only three iterations are sufficient to obtain a convergent result. The detailed electric field across a cut-plane is calculated and is presented in Fig. 7. In the simulations, the distance between the head model and the dipole antenna is set to $d = 20 \text{ mm}$ and the operating frequency is set to 900 MHz . between the hybrid NFM/MoM and the CST results for the same problem.

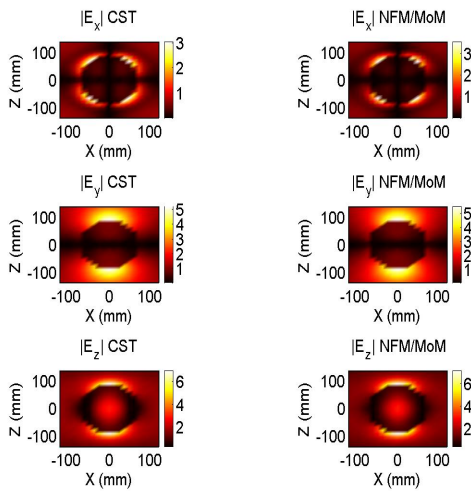


Fig. 7. Field distribution on plane $y = 4 \text{ cm}$ from the prolate shell head model adjacent to a half wavelength dipole antenna with distance 2 cm . Iteration=3.

IV. CONCLUSION

A handset antenna operating in front of a layered prolate head model was the subject of the present study. Hybrid NFM/MoM was applied to simulate the interaction of the antenna with the head model. The MoM and NFM were used to solve the source region and scatter region, respectively, and the iteration procedure was used to obtain the stable results. Numerical results show the accuracy and efficiency of the proposed hybrid method. As the analysis property of VSWF

used in NFM, the unknowns in NFM are very small, which makes the hybrid NFM/MoM be very efficient. Thus, it is easy to offer quick estimation of the field regarding the mobile terminal's position, which is very useful for optimizing the antenna to obtain a good performance.

ACKNOWLEDGMENT

This work was supported by the Shun Hing Institute of Advanced Engineering, The Chinese University of Hong Kong.

REFERENCES

- [1] *Procedure to Determine the Specific Absorption Rate (SAR) for Hand-Held Devices Used in Close Proximity to the Ear (Frequency Range of 300 MHz to 3 GHz)*, International Electrotechnical Commission (IEC) Standard 62209-1, Feb., 2005.
- [2] *IEEE Recommended Practice for Determining the Peak Spatial-Average Specific Absorption Rate (SAR) in the Human Head From Wireless Communications Devices: Measurement Techniques*, IEEE Standard 1528-2003, Dec. 2003.
- [3] S. M. Rao, D. R. Wilton, and A. W. Glisson, "Electromagnetic Scattering by Surfaces of Arbitrary Shape," *IEEE Trans. Antennas Propag.*, vol. 30, pp. 409-418, 1982.
- [4] P. J. Dimbylow and O. P. Gandhi, "Finite-difference time-domain calculations of SAR in a realistic heterogeneous model of the head for plane-wave exposure from 600 MHz to 3 GHz," *Phys. Med. Biol.*, vol. 36, no. 8, pp. 1075-1089, 1991.
- [5] M. Okoniewski and M. A. Stuchly, "A study of the handset antenna and human body interaction," *IEEE Trans. Microwave Theory Tech.*, vol. 44, pp. 1855-1864, Oct. 1996.
- [6] P. C. Waterman, "Matrix formulation of electromagnetic scattering," *Proc. IEEE* 53, 805, 1965.
- [7] P. C. Waterman, "Scattering by dielectric obstacles," *Alta Freq.* 38, 348, 1969.
- [8] P. C. Waterman, "New formulation of acoustic scattering," *J. Acoust. Soc. Am.* 45, 1417, 1969.
- [9] B. Peterson, S. Ström, "T-matrix for electromagnetic scattering from an arbitrary number of scatterers and representations of $E(3)$," *Phys. Rev.* 8, 3661, 1973.
- [10] V. K. Varadan, "Multiple scattering of acoustic, electromagnetic and elastic waves," in *Acoustic, Electromagnetic and Elastic Wave Scattering-Focus on the T-Matrix Approach*, ed. by V. K. Varadan, V. V. Varadan Pergamon, New York, pp. 103-134, 1980.
- [11] S. Ström, W. Zheng, "The null field approach to electromagnetic scattering from composite objects," *IEEE Trans. Antennas Propag.* 36, 376, 1988.
- [12] S. Makarov, "MoM Antenna Simulations with Matlab: RWG Basis.
- [13] A. Doicu, T. Wriedt, Y. A. Eremin, "Light Scattering by Systems of Particles," Springer, 2006.
- [14] P. M. Morse, H. Feshbach, "Methods of Theoretical Physics," Part 2, Chap. 13, McGraw-Hill, New York, 1953.
- [15] "CST Studio Suite 2008 User's Manual," CST GmbH, Germany, 2008.